revista mexicana de física 28 no.2 (1982) 207-224

MAGNETIZATION OF CYLINDRICAL HARD SUPERCONDUCTORS IN PERPENDICULARLY APPLIED MAGNETIC FIELDS

T. Akachi and R. Barrio

Instituto de Investigaciones en Materiales
Universidad Nacional Autónoma de México
Apartado Postal 70-360. México 20, D.F.

ABSTRACT

The magnetization of hard superconductors with cylindrical geometry when a magnetic field is applied perpendicularly to the axis of symmetry is calculated. The results are compared with those obtained[4] when the field is applied parallel to the axis of symmetry of the sample.

RESUMEN

Se hace un cálculo de la magnetización de superconductores duros con geometría cilíndrica cuando se aplica un campo magnético perpendicular al eje de simetría. Los resultados se comparan con aquéllos obtenidos[4] cuando el campo se aplica paralelamente al eje de simetría de la muestra.

I. INTRODUCTION

The knowledge of the energy losses in hard superconductors of

cylindrical geometry, with the magnetic field applied perpendicularly to the axis of symmetry of the cylindrical sample, is of a great importance, for example, in the design of superconducting magnets to generate large magnetic fields.

The first phenomenological model to explain the magnetic behavior of hard superconductors was proposed by Bean[1] and further developed by Kim, Hempstead and Strnad[2] and is known as the critical state model. Taking as the critical state equation[3]

$$J_c H_i^{\gamma} = \alpha(T) \tag{1}$$

(where the temperature dependent parameter $\alpha(T)$ is a quantity related to the pinning strength of the flux quanta and the parameter γ gives the power dependence of the critical current density J_c on the internal magnetic field H_i of the sample), Akachi et al.[4] have shown that for a cylindrical hard superconducting sample the field profile of the remanent (or trapped) magnetic flux has three possible distributions that depend on the value of the maximum applied (or peak) field H_o, as is shown schematically in Fig. 1. These three different forms of the remanent field profiles lead to three different expressions for the magnetization cycle curves.

This paper deals with the calculations of the magnetization of cylindrical hard superconducting specimens with the external field H applied perpendicularly to the axis of symmetry of the cylindrical sample. On the basis of the critical state model and using Eq. (1), the three possible types of magnetization cycle curves are calculated. The results are compared with those obtained when the field is parallel to the axis of symmetry of the cylindrical sample[4].

II. CALCULATIONS OF THE MAGNETIZATION

Let us assume a cylindrical hard superconducting sample of length L and radius R, with an external applied magnetic field H perpendicular to the axis of symmetry of the sample. We take the center point of the cylinder as the origin of coordinates, with the direction of the

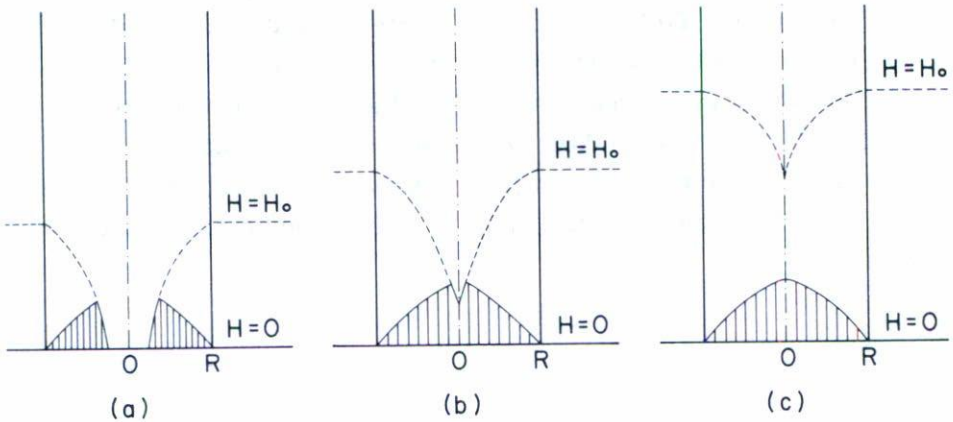

Fig. 1 Schematic representation of the three possible internal field distributions due to the remanent magnetic flux.

axis of symmetry as the Z-coordinate and the X-coordinate as the direction of H. Assuming, for simplicity, that the internal field H_i has variations only in the direction of the coordinate Y, Ampère's law for the critical state model reduces to

$$\frac{\partial H_i}{\partial y} = \begin{cases} 0, & \text{in regions where there is no field} \\ \pm \frac{4\pi}{c} J_c, & \text{in regions where there are fields} \end{cases} \qquad (2)$$

where the sign can be fixed by Lenz's law.

The magnetization is by definition

$$-4\pi M = \int (H_e - H_i)\, dV \Big/ \int dV \quad , \tag{3}$$

where both integrals are over the entire volume of the specimen and H_e is the effective magnetic field felt by the sample. In order to calculate the magnetization, we have to state H_i in terms of H and Y for each step of the magnetization cycle, and then perform the corresponding integrations of Eq. (3); this can be done by the pertinent combination of Eqs. (1) and (2). For the first stage of the magnetization, that is when in a virgin sample we increase the field starting from zero, we have from Eqs. (1) and (2)

$$H_i(Y) = \begin{cases} 0 & , \ 0 \le Y \le \Delta \\ \left[(2H)^{\gamma+1} - (\gamma+1)\frac{4\pi}{c}\alpha(R-Y) \right]^{1/(\gamma+1)} & , \ \Delta \le Y \le R \end{cases} \tag{4}$$

where we have assumed that $H_i = H_e$ at $Y = R$; on the other hand, taking into account the demagnetizing factor[5] we have that $H_e = 2H$ at $Y = R$. The parameter Δ is the so-called penetration depth and is defined as the Y-value at which H_i becomes zero, that is,

$$\Delta = R - \frac{(2H)^{\gamma+1}}{(\gamma+1)\alpha 4\pi/c} \quad . \tag{5}$$

Now, when Δ becomes zero we have that the front of the flux profile just reaches the plane $Y = 0$, and currents flow through the entire volume of the specimen. If we call H^* the field value at which this occurs, we have

$$H^* = \frac{1}{2}\left[(\gamma+1)\,\frac{4\pi}{c}\,\alpha R \right]^{1/(\gamma+1)} \quad . \tag{6}$$

It is convenient to introduce the following dimensionless variables

$$x = \frac{X}{R}\ , \qquad y = \frac{Y}{R}\ , \qquad z = \frac{Z}{L}\ ,$$
$$m = \frac{M}{H^*}\ , \qquad h = \frac{H}{H^*}\ , \qquad h_n = \frac{H_n}{H^*}\ , \tag{7}$$

where in the last relation the subscript n represents any subscript that appears in the context. Using these quantities, Eq. (3) can be written as

$$-4\pi m = \int (h_e - h_i)\, dv \Big/ \int dv\ , \tag{8}$$

where $dv = dx\, dy\, dz$. On the other hand, Eq. (4) can be written as

$$h_i(y) = \begin{cases} 0 & , \quad 0 \le y \le \delta \\ 2\left[h^{\gamma+1} - 1 + y\right]^{1/(\gamma+1)} & , \quad \delta \le y \le 1 \end{cases}\ , \tag{9}$$

where

$$\delta = \frac{\Delta}{R} = 1 - h^{\gamma+1}\ . \tag{10}$$

Substituting Eq. (9) into Eq. (8) we obtain

$$-4\pi m = 2h - \frac{8}{\pi}\int_{\delta}^{1} \left[h^{\gamma+1} - 1 + y\right]^{1/(\gamma+1)} (1-y^2)^{1/2}\, dy \tag{11}$$

for the field interval, $0 \le h \le 1$. This integral is not analytic for all values of γ and in general has to be solved numerically.

We have that the integrals that appear in the calculation of the magnetization all have the following form:

$$I_i = \int_a^b \left[A + B + Cy\right]^{1/(\gamma+1)} (1-y^2)^{1/2}\, dy\ , \tag{12}$$

where the quantity $2\left[A+B+Cy\right]^{1/(\gamma+1)}$, with the appropriate values of

the parameters A, B and C, gives the normalized internal field distribution, for some field interval, in the region $[a,b]$. The internal field distribution, for some field interval can have different distributions along the Y direction of the sample, that give rise to several integrals of the type of Eq. (12), which are distinguished by the subscript i.

a) Magnetization Cycle I

When the normalized peak field h_o is in the range $0 \leq h_o \leq 1$, the internal field distribution due to the remanent magnetic flux is like that of Fig. 1a. Let us calculate the normalized magnetization cycle corresponding to this condition. Fig. 2 illustrates schematically the normalized internal field distribution for the different stages of the magnetization cycle. Because of the symmetry, only one half of the cylinder is shown. Table I shows, for each step of the magnetization process: the corresponding field interval; the appropriate integrals I_i, along with the values of the limits of integration $[a,b]$ and the values of the parameters A, B and C; and the corresponding expression for the magnetization. The parameters δ_o, δ' and δ'_o that appear both in Fig. 2 and Table I have the following expressions:

$$\delta_o = 1 - h_o^{\gamma+1} \quad , \tag{13}$$

$$\delta' = 1 - \frac{1}{2}\left(h_o^{\gamma+1} - h^{\gamma+1}\right) \quad , \tag{14}$$

$$\delta'_o = 1 - \frac{1}{2}h_o^{\gamma+1} \quad . \tag{15}$$

Fig. 3 shows a curve of a magnetization cycle, calculated by the expressions of Table I, for the case when $\gamma = 0.5$ and $h_o = 0.8$.

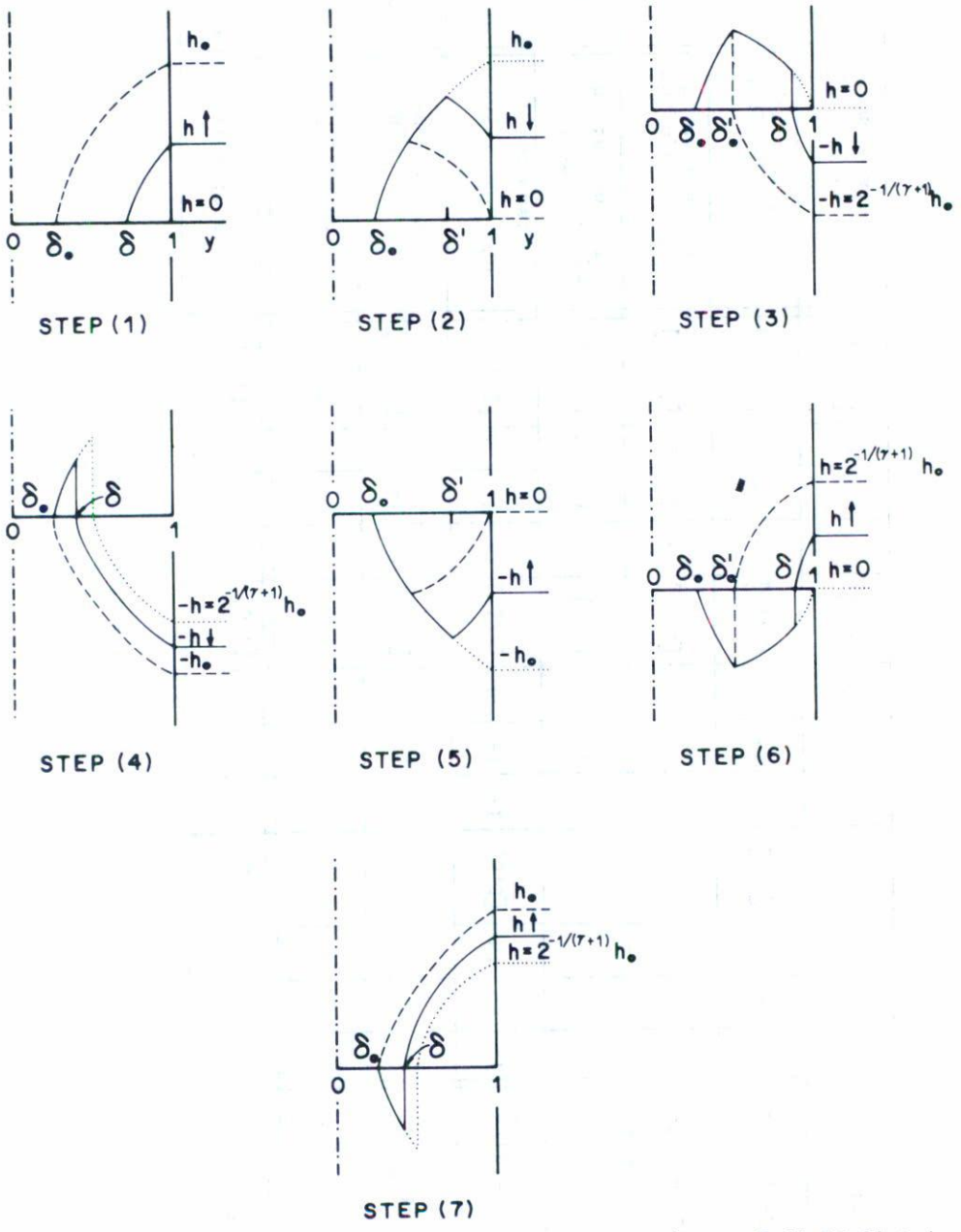

Fig. 2 Schematic representation of the normalized internal field distribution for the different stages of the magnetization cycle for the case when $0 \leq h_o \leq 1$. (Because of the symmetry only one half of the cylinder is shown). In each one of the step figures the dotted line represents the initial state, the dashed line the final state and the full line an intermediate state.

TABLE I

Magnetization Cycle I. $0 \leq h_o \leq 1$.

Step	Field Interval	I_1				I_2				I_3				$-4\pi m$
		$[a,b]$	A	B	C	$[a,b]$	A	B	C	$[a,b]$	A	B	C	
1	$0 \leq h \leq h_o$ h increasing	$[\delta,1]$	h	-1	+1									$2h - \frac{8}{\pi} I_1$
2	$h_o \leq h \leq 0$ h decreasing	$[\delta_o,\delta']$	h_o	-1	+1	$[\delta',1]$	h	+1	-1					$2h - \frac{8}{\pi}(I_1+I_2)$
3	$0 \leq h \leq -2^{-1/(\gamma+1)} h_o$ $\lvert h\rvert$ increasing	$[\delta_o,\delta_o']$	h_o	-1	+1	$[\delta_o',\delta]$	0	+1	-1	$[\delta,1]$	$\lvert h\rvert$	-1	+1	$-2\lvert h\rvert - \frac{8}{\pi}(I_1+I_2-I_3)$
4	$-2^{-1/(\gamma+1)} h_o \leq h \leq -h_o$ $\lvert h\rvert$ increasing	$[\delta_o,\delta]$	h_o	-1	+1	$[\delta,1]$	$\lvert h\rvert$	-1	+1					$-2\lvert h\rvert - \frac{8}{\pi}(I_1-I_2)$
5	$-h_o \leq h \leq 0$ $\lvert h\rvert$ decreasing	$[\delta_o,\delta']$	h_o	-1	+1	$[\delta',1]$	$\lvert h\rvert$	+1	-1					$-2\lvert h\rvert + \frac{8}{\pi}(I_1+I_2)$
6	$0 \leq h \leq 2^{-1/(\gamma+1)} h_o$ h increasing	$[\delta_o,\delta_o']$	h_o	-1	+1	$[\delta_o',\delta]$	0	+1	-1	$[\delta,1]$	h	-1	+1	$2h + \frac{8}{\pi}(I_1+I_2-I_3)$
7	$2^{-1/(\gamma+1)} h_o \leq h \leq h_o$ h increasing	$[\delta_o,\delta]$	h_o	-1	+1	$[\delta,1]$	h	-1	+1					$2h + \frac{8}{\pi}(I_1-I_2)$

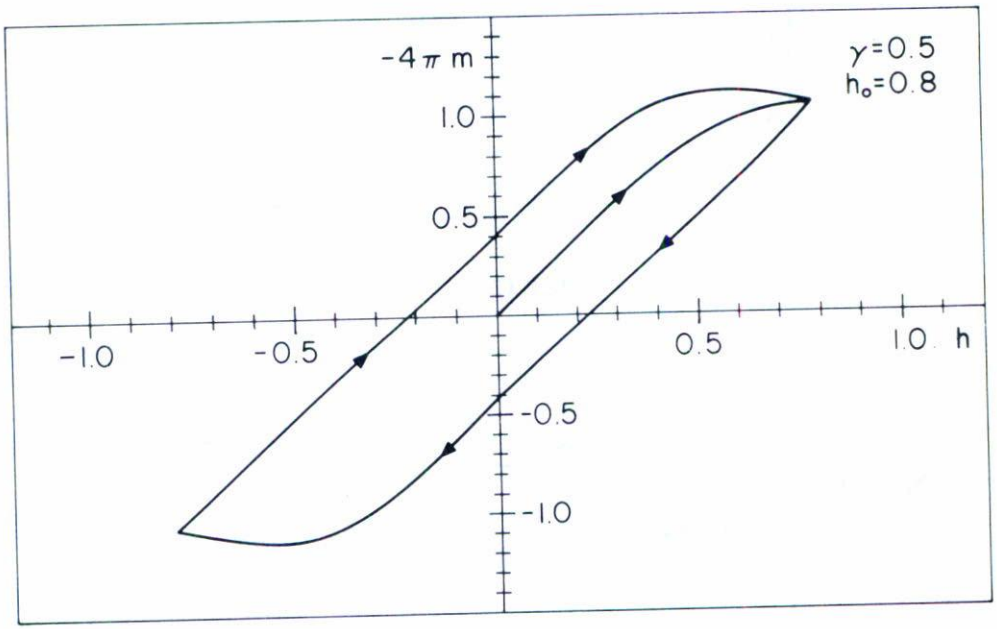

Fig. 3 Normalized magnetization cycle curve for $\gamma = 0.5$ and $h_o = 0.8$.

b) Magnetization Cycle II

This magnetization cycle occurs when h_o is in the range $1 \leq h_o \leq 2^{1/(\gamma+1)}$, which gives rise to an internal field distribution for the remanent magnetic flux like that of Fig. 1b. The normalized internal field distribution for this case is illustrated schematically, step by step, in Fig. 4 (because of the symmetry only one half of the cylinder is shown). Table II shows, for each step: the field interval, the appropriate integrals I_i and the expression for the magnetization. The expressions for δ, δ' and δ'_o are given by Eqs. (10), (14) and (15), respectively. A complete normalized magnetization cycle for $\gamma = 0.75$ and $h_o = 1.25$ is shown in Fig. 5.

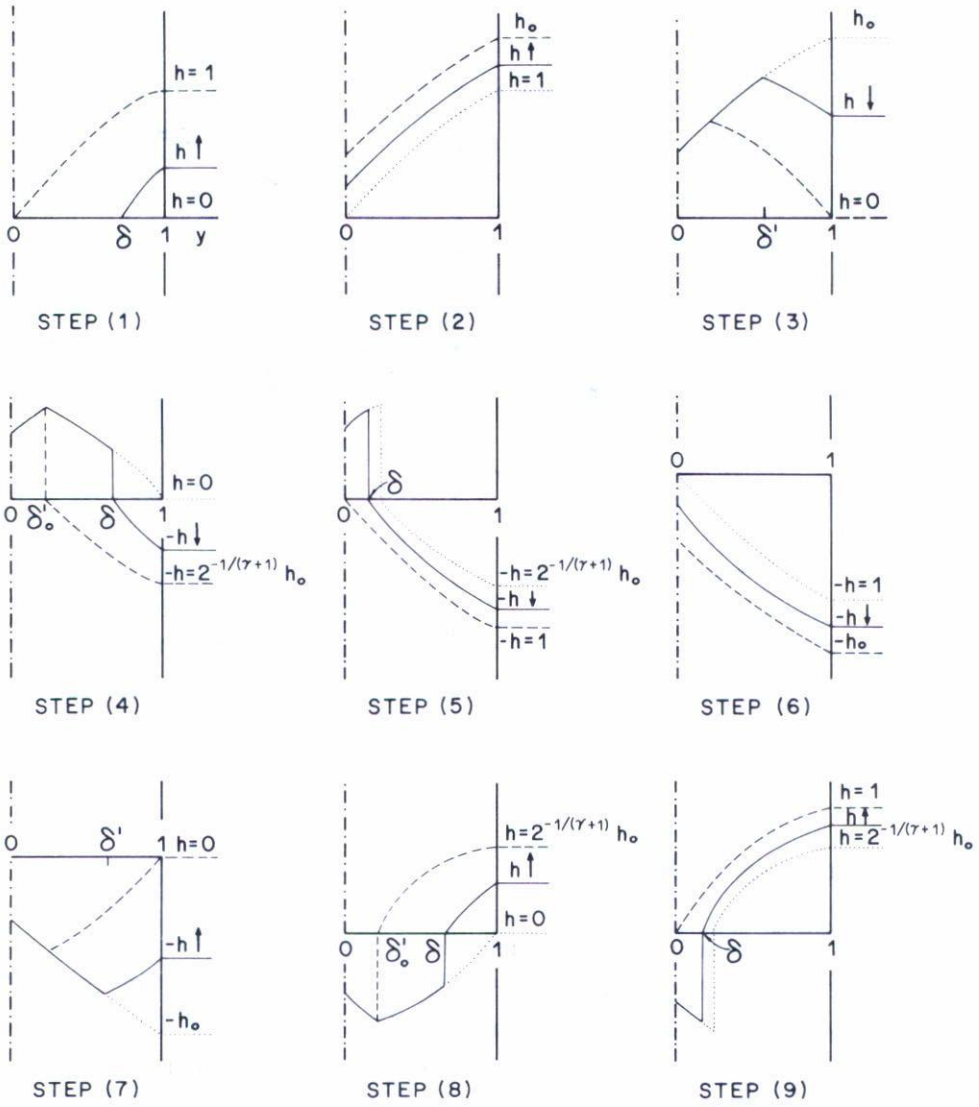

Fig. 4 Schematic representation of the normalized internal field distribution for the different stages of the magnetization cycle for the case when $1 \leq h_o \leq 2^{1/(\gamma+1)}$. (Because of the symmetry only one half of the cylinder is shown). In each one of the step figures the dotted line represents the initial state, the dashed line the final state and the full line an intermediate state.

TABLE II

Magnetization Cycle II. $1 \le h_o \le 2^{1/(\gamma+1)}$.

Step	Field Interval	I_1				I_2				I_3				$-4\pi m$
		$[a,b]$	A	B	C	$[a,b]$	A	B	C	$[a,b]$	A	B	C	
1	$0 \le h \le 1$ h increasing	$[\delta,1]$	h	-1	+1									$2h-\frac{8}{\pi}I_1$
2	$1 \le h \le h_o$ h increasing	$[0,1]$	h	-1	+1									$2h-\frac{8}{\pi}I_1$
3	$h_o \le h \le 0$ h decreasing	$[0,\delta']$	h_o	-1	+1	$[\delta',1]$	h	+1	-1					$2h-\frac{8}{\pi}(I_1+I_2)$
4	$0 \le h \le -2^{-1(\gamma+1)}h_o$ $\lvert h\rvert$ increasing	$[0,\delta_o']$	h_o	-1	+1	$[\delta_o',\delta]$	0	+1	-1	$[\delta,1]$	$\lvert h\rvert$	-1	+1	$-2\lvert h\rvert-\frac{8}{\pi}(I_1+I_2-I_3)$
5	$-2^{-1/(\gamma+1)}h_o \le h \le -1$ $\lvert h\rvert$ increasing	$[0,\delta]$	h_o	-1	+1	$[\delta,1]$	$\lvert h\rvert$	-1	+1					$-2\lvert h\rvert-\frac{8}{\pi}(I_1-I_2)$
6	$-1 \le h \le -h_o$ $\lvert h\rvert$ increasing	$[0,1]$	$\lvert h\rvert$	-1	+1									$-2\lvert h\rvert+\frac{8}{\pi}I_1$
7	$-h_o \le h \le 0$ $\lvert h\rvert$ decreasing	$[0,\delta']$	h_o	-1	+1	$[\delta',1]$	$\lvert h\rvert$	+1	-1					$-2\lvert h\rvert+\frac{8}{\pi}(I_1+I_2)$
8	$0 \le h \le 2^{-1/(\gamma+1)}h_o$ h increasing	$[0,\delta_o']$	h_o	-1	+1	$[\delta_o',\delta]$	0	+1	-1	$[\delta,1]$	h	-1	+1	$2h+\frac{8}{\pi}(I_1+I_2-I_3)$
9	$2^{-1/(\gamma+1)}h_o \le h \le 1$ h increasing	$[0,\delta]$	h_o	-1	+1	$[\delta,1]$	h	-1	+1					$2h+\frac{8}{\pi}(I_1-I_2)$

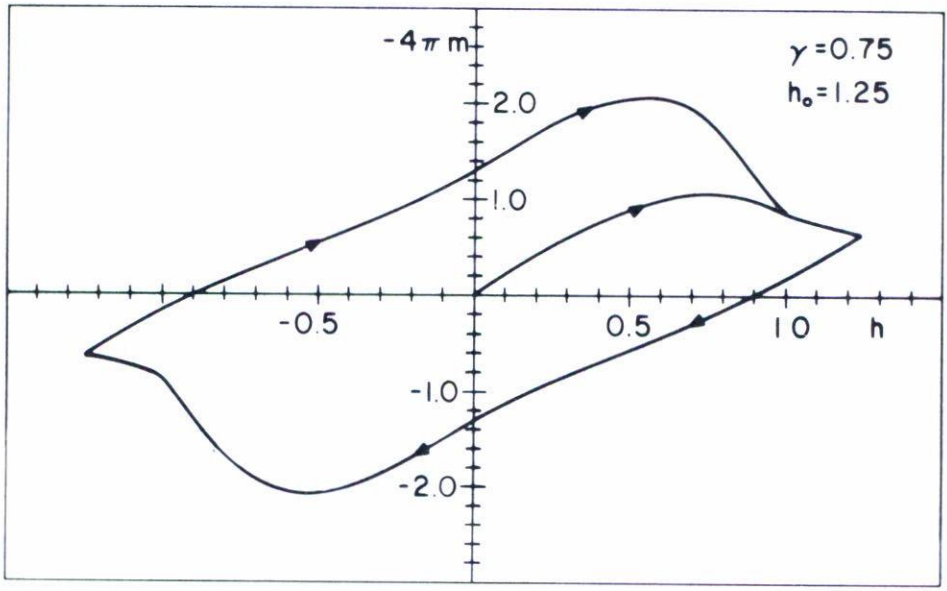

Fig. 5 Normalized magnetization cycle curve for $\gamma = 0.75$ and $h_o = 1.25$.

c) *Magnetization Cycle III*

When $2^{1/(\gamma+1)} \leq h_o << h_{c2}$, where h_{c2} is the normalized upper critical magnetic field, the internal field distribution for the remanent magnetic flux is like that of Fig. 1c. The normalized internal field distribution for this cycle is illustrated in Fig. 6. The field interval, the integrals I_i and the expression for the magnetization for each step of the magnetization cycle are shown in Table III. Fig. 7 shows a normalized magnetization cycle for $\gamma = 1.0$ and $h_o = 2.0$.

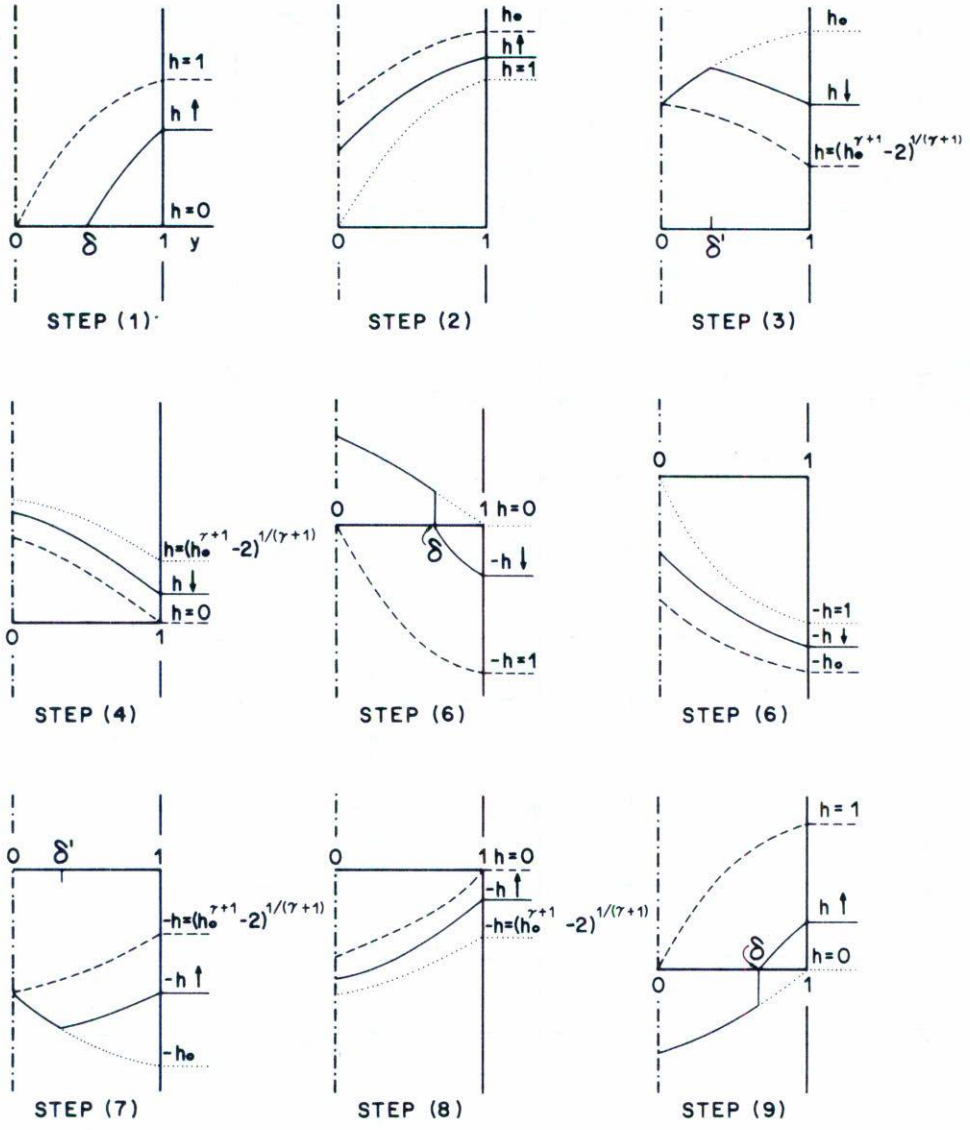

Fig. 6 Schematic representation of the normalized internal field distribution for the different stages of the magnetization cycle for the case when $2^{1/(\gamma+1)} \leq h_o << h_{c2}$. (Because of the symmetry only one half of the cylinder is shown). In each one of the step figures the dotted line represents the initial state, the dashed line the final state and the full line an intermediate state.

TABLE III

Magnetization Cycle III. $2^{1/(\gamma+1)} \leq h_o << h_{c2}$.

Step	Field Interval	I_1				I_2				$-4\pi m$
		$[a,b]$	A	B	C	$[a,b]$	A	B	C	
1	$0 \leq h \leq 1$ h increasing	$[\delta,1]$	h	-1	+1					$2h - \frac{8}{\pi} I_1$
2	$1 \leq h \leq h_o$ h increasing	$[0,1]$	h	-1	+1					$2h - \frac{8}{\pi} I_1$
3	$h_o \leq h \leq (h_o^{\gamma+1}-2)^{1/(\gamma+1)}$ h decreasing	$[0,\delta']$	h_o	-1	+1	$[\delta',1]$	h	+1	-1	$2h - \frac{8}{\pi}(I_1+I_2)$
4	$(h_o^{\gamma+1}-2)^{1/(\gamma+1)} \leq h \leq 0$ h decreasing	$[0,1]$	h	+1	-1					$2h - \frac{8}{\pi} I_1$
5	$0 \leq h \leq -1$ $\lvert h \rvert$ increasing	$[0,\delta]$	0	+1	-1	$[\delta,1]$	$\lvert h \rvert$	-1	+1	$-2\lvert h \rvert - \frac{8}{\pi}(I_1-I_2)$
6	$-1 \leq h \leq -h_o$ $\lvert h \rvert$ increasing	$[0,1]$	$\lvert h \rvert$	-1	+1					$-2\lvert h \rvert + \frac{8}{\pi} I_1$
7	$-h_o \leq h \leq -(h_o^{\gamma+1}-2)^{1/(\gamma+1)}$ $\lvert h \rvert$ decreasing	$[0,\delta']$	h_o	-1	+1	$[\delta',1]$	$\lvert h \rvert$	+1	-1	$-2\lvert h \rvert + \frac{8}{\pi}(I_1+I_2)$
8	$-(h_o^{\gamma+1}-2)^{1/(\gamma+1)} \leq h \leq 0$ $\lvert h \rvert$ decreasing	$[0,1]$	$\lvert h \rvert$	+1	-1					$-2\lvert h \rvert + \frac{8}{\pi} I_1$
9	$0 \leq h \leq 1$ h increasing	$[0,\delta]$	0	+1	-1	$[\delta,1]$	h	-1	+1	$2h + \frac{8}{\pi}(I_1-I_2)$

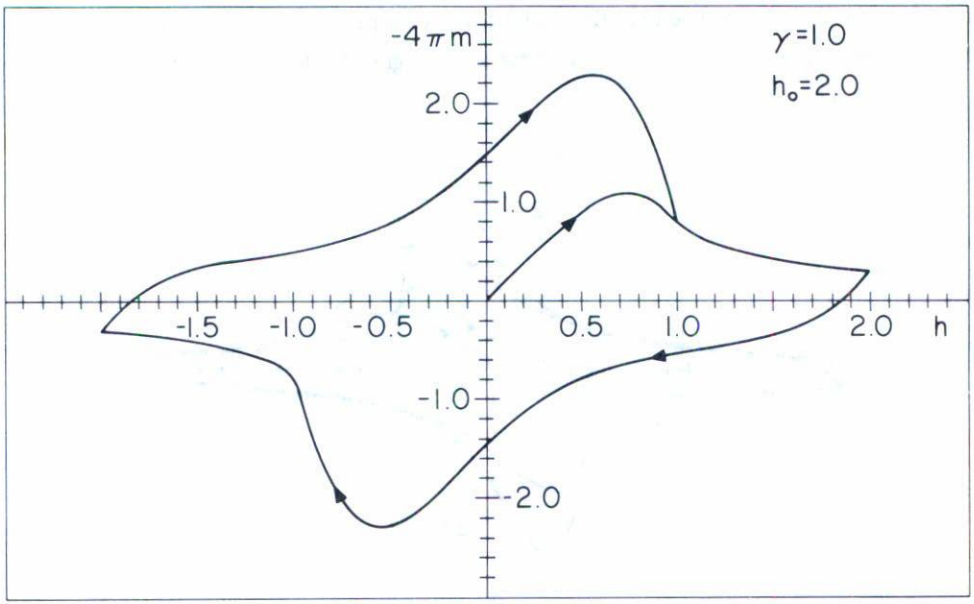

Fig. 7 Normalized magnetization cycle curve for $\gamma = 1.0$ and $h_o = 2.0$.

III. COMPARISON OF THE MAGNETIZATION CURVES FOR PERPENDICULARLY AND LONGITUDINALLY APPLIED FIELDS

In this section we compare the magnetization curves obtained when the field is applied perpendicularly to the axis of symmetry of a cylindrical sample (perpendicular case) with those when the field is applied longitudinally to the same axis (parallel case). The expressions for the magnetization for the latter case can be found in reference 4.

In order to compare the magnetization curves we have to use, in both cases, the same normalization factor; we have used Eq. (6) as this factor. Fig. 8 shows the magnetization curves, calculated for $\gamma = 1.0$ and $h_o = 3.6$, for the perpendicular (dashed line) and the parallel (full line) cases. We see (Fig. 8) the following general features: (a) All maxima (and minimum) in a magnetization cycle curve of the perpendicular case occur at absolute field values lower than those for the corresponding curve of the parallel case. (b) All absolute magnetization values of the maxima (and minimum) in the perpendicular case are larger than those cor-

responding to the parallel case. (c) The remanent magnetization is always larger in the perpendicular case; an example is given in Fig. 9 which shows, for both cases, the remanent magnetization as a function of h_o when $\gamma = 1.0$.

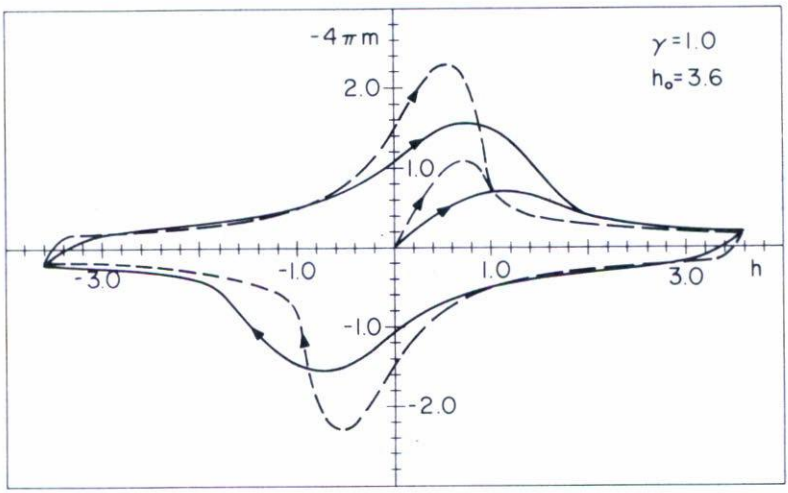

Fig. 8 Normalized magnetization cycle curve for the perpendicular (dashed line) and parallel (full line) cases when $\gamma = 1.0$ and $h_o = 3.6$.

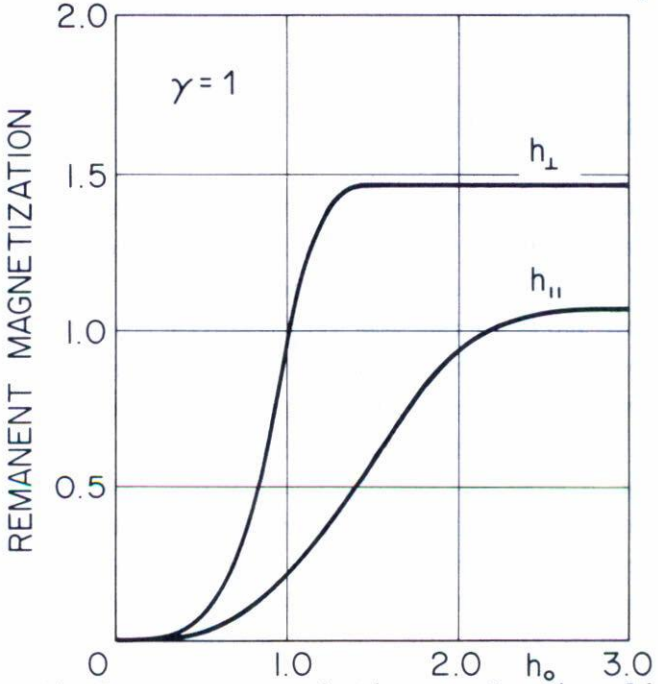

Fig. 9 The normalized remanent magnetization as a function of h_o for the perpendicular and parallel cases when $\gamma = 1.0$.

IV. CONCLUSIONS

We have calculated, using the relation $J_c H_i^{\gamma} = \alpha(T)$ as the critical state equation, the three possible magnetization cycles for hard superconducting specimens with cylindrical geometry, when the external magnetic field H is applied perpendicularly to the axis of symmetry of the sample. As was mentioned in the preceding section, the comparison of the magnetization curves between the perpendicular and parallel cases shows some differences; fundamentally, these differences come from the demagnetizing effects. On the other hand, we find in the perpendicular case, as in the parallel case[4], that (see Fig. 10), (a) the fall off of the magnetization curve after passing through its maximum, (b) the field values at which the maxima (and minimum) of the magnetization curve occur, (c) the values of the maxima (and minimum) of the magnetization and (d) the remanent magnetization, all have a strong dependence on the parameter γ.

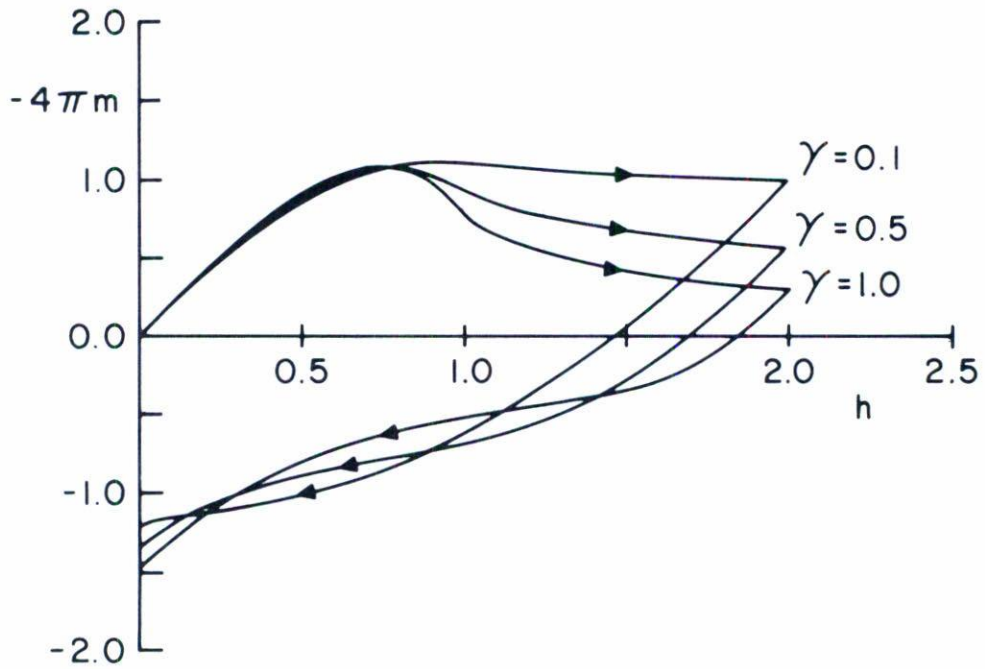

Fig. 10 Three normalized magnetization curves, corresponding to $\gamma = 0.1$, $\gamma = 0.5$ and $\gamma = 1.0$

REFERENCES

1. C.P. Bean, Phys. Rev. Letters,8 (1962) 250; Rev. Mod. Phys., 36 (1964) 31.
2. Y.B. Kim, C.F. Hempstead and A.R. Strnad, Phys. Rev., 129 (1963) 528.
3. F. Irie and K. Yamafuji, J. Phys. Soc. Japan, 23 (1967) 225.
4. T. Akachi, R. Barrio and G. Ramírez, Rev. Mex. Fís. 27 (1981) 143.
5. See, for example, A.C. Rose-Innes and E.H. Rhoderick, Introduction to Superconductivity, Pergamon Press (1969) Chap. 6.